Arabian Journal of Chemistry (2021) **14**, 102928

King Saud University

Arabian Journal of Chemistry

www.ksu.edu.sa
www.sciencedirect.com

ORIGINAL ARTICLE

Molecular imprinted polymer for β-carotene for application in palm oil mill effluent treatment

Warda Mohamed Altogbia [a], Nor Azah Yusof [a,b,*], Zulkarnain Zainal [a], Azni Idris [c], Siti Khadijah Ab Rahman [b,d], Siti Fatimah Abd Rahman [b], Azizul Isha [e,*]

[a] *Chemistry Department, Faculty of Science, Universiti Putra Malaysia, 43400 UPM Serdang, Selangor, Malaysia*
[b] *Institute of Advanced Technology, Universiti Putra Malaysia, 43400 UPM Serdang, Selangor, Malaysia*
[c] *Chemical Engineering and Environmental Department, Faculty of Engineering, Universiti Putra Malaysia, 43400 UPM Serdang, Selangor, Malaysia*
[d] *Research and Innovation Division, National Sport Institute of Malaysia, 57000 Kuala Lumpur, Malaysia*
[e] *Natural Medicines and Products Research Laboratory, Institute of Bioscience, Universiti Putra Malaysia, 43400 UPM Serdang, Selangor, Malaysia*

Received 25 August 2020; accepted 29 November 2020
Available online 3 December 2020

KEYWORDS

β-Carotene;
β-Cyclodextrin;
Molecular imprinted polymer;
Palm oil mill effluent

Abstract Palm oil mill effluent (POME) is one of the most significant pollutant in the form of wastewater. It could have negative effects on the environment include the emission of biogas and water pollution which comes from discharging the brownish tick POME to the water bodies if not properly managed. Discharge of dark brownish colored of POME directly into water bodies may affect the aquatic life as it will reduce sunlight penetration and suppress the photosynthetic activity. A molecularly imprinted polymer (MIP) for removal of β-carotene from POME has been aimed to develope in this study. The preparation of β-carotene imprinted and non-imprinted polymer (NIP) involves polymerization of β-carotene (or without it) with β-cyclodextrin (β-CD), 9-vinylcarbazole (9VC), tolylene diisocyanate (TDI) and N,N-dimethylformamide (DMF) as the monomer, co-monomer, cross-linker and solvent (porogen), respectively. Analysis from FTIR showed that MIP and NIP have similar characteristic peak with different peaks intensity, indicating the similarity in the backbone structure of polymerization. TGA result displayed high thermal stability with final decomposition at 320 °C for MIP-β-CD-9VC as compared to NIP-β-CD-9VC. The pH study shows that sorption of β-carotene increased with decreasing the pH of POME and the maximum sorption capacities achieved at pH 2 were 10 μg/g and 7 μg/g for MIP-β-CD-9VC and

* Corresponding authors at: Chemistry Department, Faculty of Science, Universiti Putra Malaysia, 43400 UPM Serdang, Selangor, Malaysia. Functional Devices Laboratory, Institute of Advanced Technology, Universiti Putra Malaysia, 43400 UPM Serdang, Selangor, Malaysia. Natural Medicines and Products Research Laboratory, Institute of Bioscience, Universiti Putra Malaysia, 43400 UPM Serdang, Selangor, Malaysia.
E-mail addresses: azahy@upm.edu.my (N.A. Yusof), azizul_isha@upm.edu.my (A. Isha).

Peer review under responsibility of King Saud University.

Production and hosting by Elsevier

https://doi.org/10.1016/j.arabjc.2020.102928

NIP-β-CD-9VC, respectively. The maximum sorption achieved by using 500 mg of MIP as the sorption of β-carotene increased with increasing the dosage of MIP. Kinetic model evaluation has been applied on this prepared materials. The sorption equilibrium data was well described by Freundlich model. The results indicated that the sorption of β-carotene on MIP follows a pseudo–second–order kinetic.

1. Introduction

Substantial contribution has been made by palm oil industries towards economic growth as well as rise in standard of living amongst the South East Asian countries. However, it is also known for being a major contributor in discharging palm oil mills effluent (POME), the largest form of pollution load (Abdulsalam et al., 2020; Tabassum et al., 2015). Almost 5–7.5 tonnes of water is needed to produce 1 tonne of crude palm oil, and greater than 50% of water converts (POME) (Wu et al., 2007).

POME is acidic in nature with a pH between 4 and 5, biological oxygen demand (BOD) of 25,000–60,000 mg L^{-1} and chemical oxygen demand (COD) of 40,000 –100,000 mg L^{-1}. The effluent's color is attributed to the presence of organic matters like phenolics, lignin, and carotenes (Bello et al., 2013; Ahmed et al., 2015). The discharge standard is not met by POME that has very dark color since it is a key contributor to pollution load in ground water. The discharged effluent's major constituent has long been the color, which needs to be eliminated for aesthetic as well as environmental reasons. Also, adverse impact can be cast on aquatic lives due to the discharging of brownish wastewater into water bodies as the color is responsible for filtering the light passing into the water. This leads to decrease photosynthesis activity as well as less quantity of dissolved oxygen. To avoid such an adverse effect, before discharging into the environment occurs, the colour needs to be removed from POME (Jasni et al., 2020; Ratpukdi, 2012).

Membrane filtration, advanced oxidation process, adsorption, ion exchange, and ozonation are some of the technologies employed in removing the colour from POME (Zahrim, 2014). Amongst these methods, adsorption is considered the most versatile and frequently employed technique because of its simplicity of design, low initial cost, and insensitivity to toxicity and ease of operation. Research works have been carried out to evaluate several adsorbents and their ability to remove color from POME, like agricultural waste and activated carbon silica particles (Aziz et al., 2020; Neoh et al., 2014). However, these adsorbents have limited ability with regards to achieve the desired objectives because of their selectivity and specificity properties. Moreover, reusability of the adsorbents has not been extensively researched. In the recent past, much popularity was attracted by the use of molecularly imprinted polymer (MIP) in treating wastewater. MIPs are synthetic antibody mimics which are synthesized through polymerization to create specific binding sites with memory of the template molecules during the synthetic process of polymers (Mosbach and Ramstrom, 1996). Molecular imprinting techniques based on MIPs has been widely used in separation, solid phase extraction, chromatography, sensors, catalysis, immunoassay and drug delivery (Wang et al., 2019).

Molecular imprinting is a powerful technique, which confers specific binding properties to synthetic polymers. The MIP synthesis comprises monomers' assembly crosslinking around the template molecules, and then polymerization alongside a cross-linker (Hegazy et al., 2016). Then, the template molecules are removed and the polymer matrix contains cavities with recognition binding sites, in which rebinding of a specific target analyte or group (structurally related analytes) can be done when extracting from real environmental samples (Ncube et al., 2017). Chemical and mechanical stabilities, high selectivity and reusability and low cost and ease of preparation are some of the advantages of MIP (Hassan et al., 2016; Yan and Row, 2006). Non-covalent imprinting is the most commonly employed technique for preparing MIP. In this process, non-covalent interactions, like electrostatic forces, hydrogen bonding, hydrophobic interactions or van der Waals forces, help in forming the complex of template and functional monomer in situ (Lafarge et al., 2020; Speltini et al., 2017).

Various analytical methods such as mass spectrometry, have been reported for the quantification of pollutants in different samples. Despite direct detection methods can enhance throughput and minimize errors associated with sample handling, low analyte concentrations, and sample complexity limit their accuracy and suitability (Azizi et al., 2020). Therefore, this study aimed to develop a selective MIP for removal of β-carotene from POME using bulk polymerization method with good adsorption capacity. Beta-cyclodextrin (β-CD) and 9-vinylcarbazole (9VC) were dissolved in N,N-dimethyl formamide (DMF) and added with β-carotene, benzoyl peroxide, and tolylene-2,4-diisocyanate (TDI) as template, initiator, and cross-linker respectively. Scheme 1 shows the schematic diagram for MIP-β-CD-9VC preparation. The polymers obtained were characterized by Fourier transform infrared spectroscopy (FTIR), thermogravimetric analysis (TGA) and field emission scanning electron microscope (FESEM). The adsorption model of β-carotene onto the imprinted and the non-imprinted materials were assessed by adsorption isotherms and the adsorption kinetic parameters were determined through kinetic measurements.

2. Experimental

2.1. Materials

β-CD, β-carotene, and TDI were procured from Sigma Aldrich (St. Louis, MO, USA). 9VC was procured from Fluka (Steinheim, Germany). Acetone, benzoyl peroxide (BPO) and DMF were procured from R&M Chemicals (Essex, UK). *n*-Hexane was procured from Bendosen and methanol was obtained from HmbG Chemicals. Real sample (POME) was collected from Pakar Go Green.

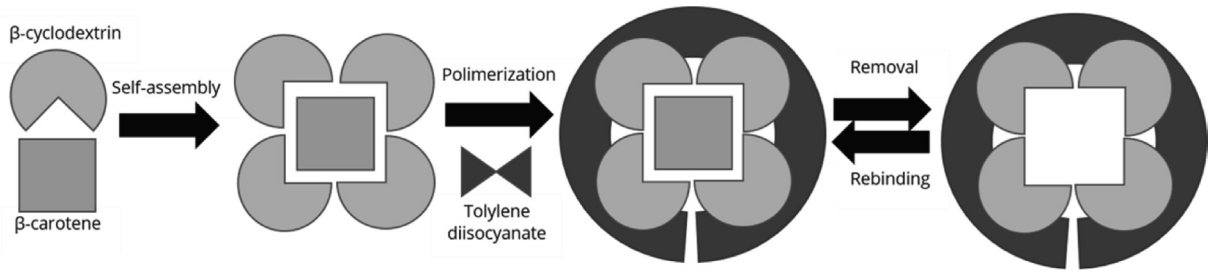

Scheme 1 Schematic diagram for MIP-β-CD-9VC preparation.

2.2. Preparation of MIP-β-CD-9VC and NIP-β-CD-9VC

The bulk polymerization method was used to prepare MIP-β-CD-9VC by dissolving 0.55 g of functional monomer, β-cyclodextrin (0.48 mmol) in 5 mL of DMF, followed by the addition of 0.5 g co-monomer, 9-vinylcarbazole (2.58 mmol) and 0.05 g of β-carotene (0.1 mmol). 4.0 mL of cross-linker, TDI (27.8 mmol) and 0.03 g of initiator, BPO were added to the mixture. The mixture was sonicated using sonicator for 15 min until completely dissolved. Then the mixture was purged with nitrogen gas for 10 min followed by placing in water bath at 70 °C for 3 h. NIP-β-CD-9VC was prepared exactly the same procedure as-described above, but without the β-carotene template. The obtained polymers were crush, ground and sieved through a 90 μm stainless steel mesh. The sieved particles were washed with a mixture of *n*-hexane–acetone (1:1, v/v) until no template was detected using UV spectroscopy. The synthesized polymers were dried in a vacuum drying oven (60 ℃) until a constant weight and stored at 4℃ for the further analysis.

2.3. Characterization of MIP-β-CD-9VC and NIP-β-CD-9VC

FTIR spectra for the MIP-β-CD-9VC and NIP-β-CD-9VC were recorded using FTIR Perkin Elmer 1600 Spectrophotometer. The thermal analysis of the MIP-β-CD-9VC and NIP-β-CD-9VC were carried out using a Mettler Toledo Star SW 7.01. The surface morphology of the MIP-β-CD-9VC and NIP-β-CD-9VC were examined using FESEM system (FEI NANOSEM 230).

2.4. Adsorption studies

The adsorption capacity study of the polymer was done by adding 0.2 g of MIP-β-CD-9VC and NIP-β-CD-9VC particles into10 mL of POME mixed solution of methanol–water (1:1, v/v). The resulting supernatant was measured for unbound β-carotene by UV spectrometry at λ max = 450 nm. The adsorption capacity of adsorbents was calculated as below (Rahman et al., 2018):

$$q = \frac{(C_0 - C_e) \times V}{M} \tag{1}$$

where q (mg g^{-1}) represents the amount of total adsorption of β-carotene, C_o and C_e signify initial and equilibrium concentrations of β-carotene in POME (mg L^{-1}), M (g) indicates the weight of adsorbents and V (L) denotes the volume of the POME sample.

The optimum pH for adsorption of β-carotene was studied by using different pH value ranging from 2.0 to 9.0. The effect of dosage was studied by varying the dosage of MIP-β-CD-9VC from 0.05 to 0.50 g. The sorption isotherm was measured by applying different concentrations of POME solution ranging from 0.1 to 2.5 mg L^{-1}. Effect of time was studied by collected the POME solution at different time intervals. The maximum time required for maximum adsorption of β-carotene was determined from the plot of adsorption capacity of β-carotene (mg g^{-1}) versus time (minutes). The reusability study of MIP-β-CD-9VC was evaluated for 5 cycles. After each test, the MIP-β-CD-9VC was rinsed with a mixture of *n*-hexane–acetone (1:1, v/v), and subsequently it was reused for the next test cycle. The filtrate was analyzed using UV spectrometer.

The Langmuir and Freundlich model were used to describe the equilibrium data for the adsorption of β-carotene on MIP-β-CD-9VC. The Langmuir model may be depicted in a linear equation form as follows (Choong et al., 2010):

$$\frac{C_e}{q_e} = \frac{C_e}{Q_m} + \frac{1}{bQ_m} \tag{2}$$

where C_e represents the equilibrium concentration (mg L^{-1}), q_e represents the quantity of β-carotene adsorbed during equilibrium (mg g^{-1}), and Q_m and b represent Langmuir constants, which are associated with the sorption capacity and energy

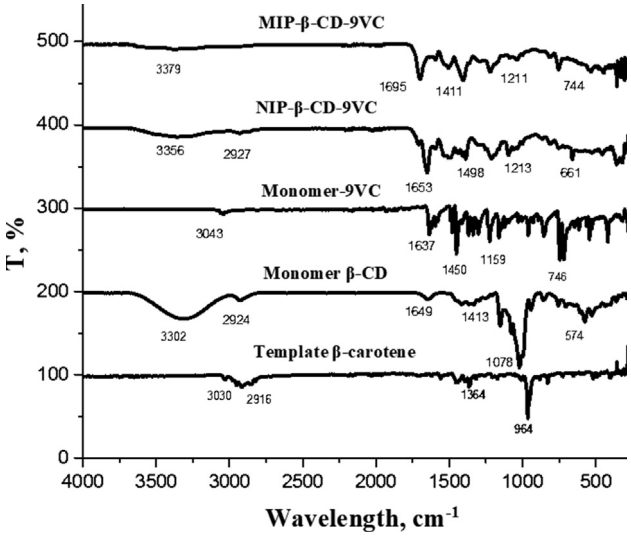

Fig. 1 FTIR for template β-carotene, monomer β-CD, monomer-9VC, MIP-β-CD-9VC and NIP-β-CD-9VC.

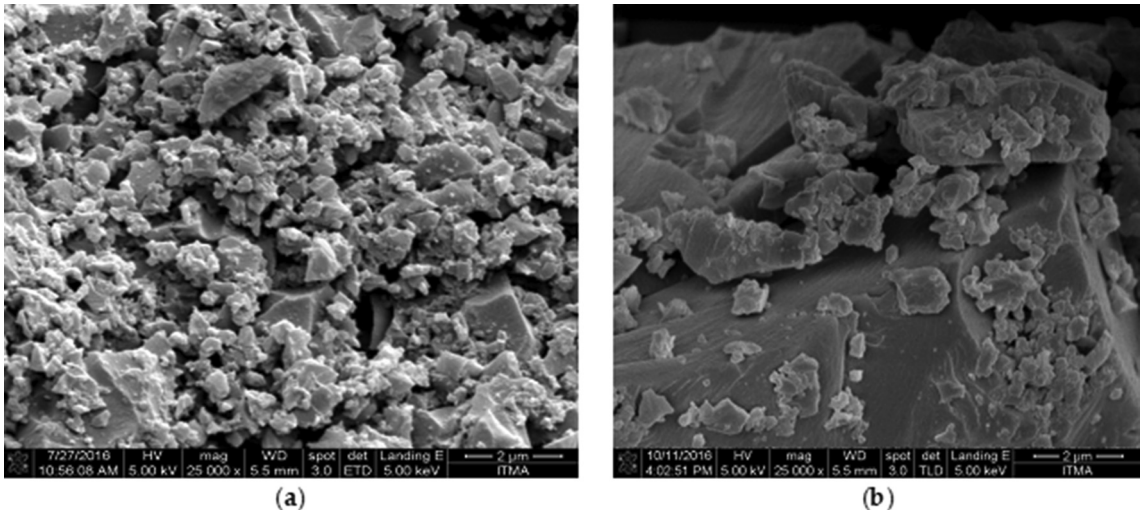

Fig. 2 FESEM image of (a) MIP-β-CD-9VC and (b) NIP-β-CD-9VC.

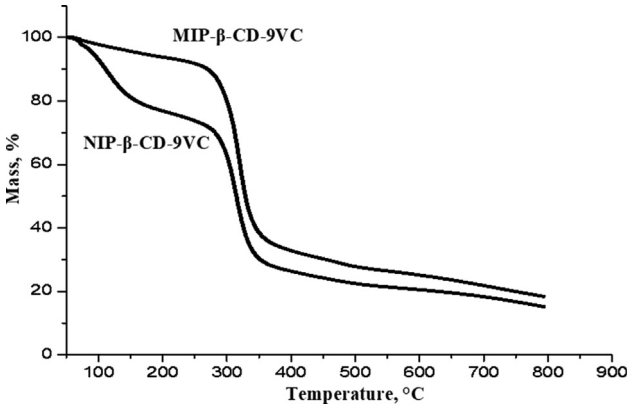

Fig. 3 TGA curve for MIP-β-CD-9VC and NIP-β-CD-9VC.

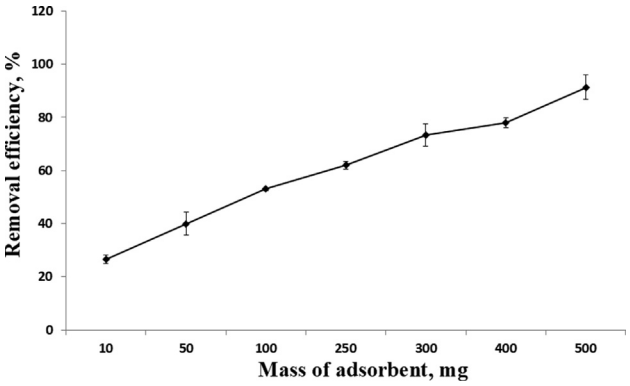

Fig. 5 Removal percentage of β-carotene for different dosages of MIP-β-CD-9VC (Experimental conditions: pH 2; POME concentration solution, 2.5 mg L^{-1}; contact time, 20 min).

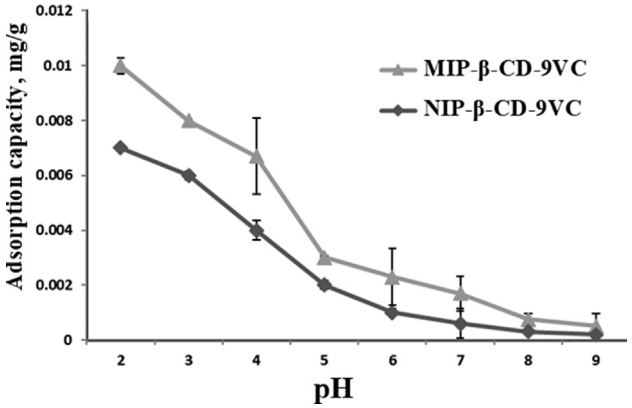

Fig. 4 Comparison of the effect of pH on the adsorption of β-carotene by the MIP-β-CD-9VC and NIP-β-CD-9VC particles (Experimental conditions: POME concentration solution, 2.5 mg L^{-1}; polymer dosage, 500 mg; contact time, 20 min).

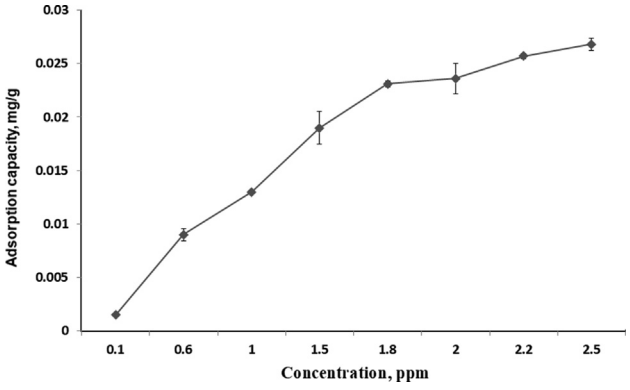

Fig. 6 The adsorption capacity of various concentrations of β-carotene by MIP-β-CD-9VC (Experimental conditions: pH 2; polymer dosage, 500 mg; contact time, 20 min).

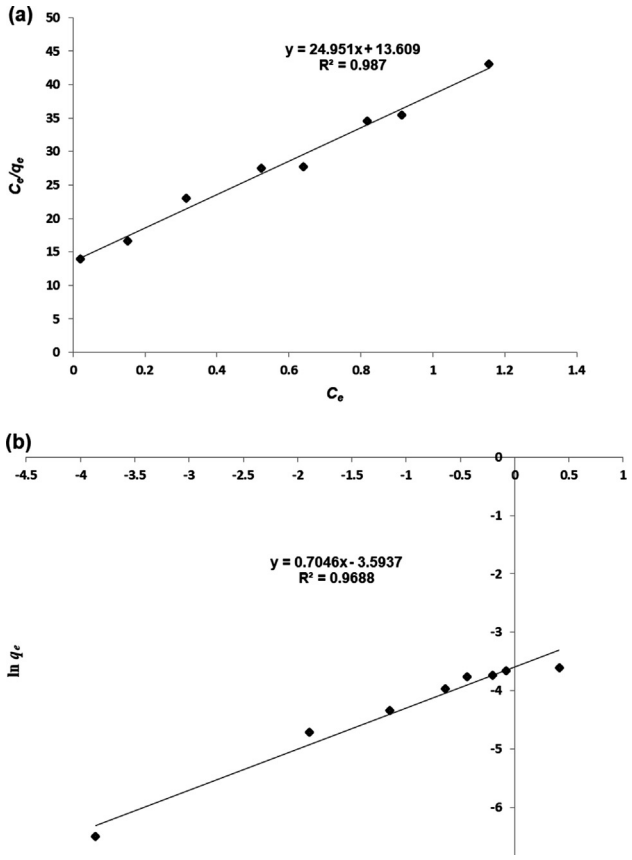

Fig. 7 (a) Langmuir plot and (b) Freundlich plot for the adsorption of β-carotene by MIP-β-CD-9VC. (Experimental conditions: pH 2; POME concentration solution, 2.5 mg L^{-1}; polymer dosage, 500 mg; contact time, 20 min).

of sorption, respectively. The Langmuir isotherm was validated using the plot of C_e/q_e against C_e.

The Freundlich isotherm is considered as an exponential equation. Thus, there is an assumption that an increase in the sorbate concentration results into an increase in the sorbate concentration on the adsorbent surface. The equation below is a frequently utilized linear equation for the Freundlich isotherm (Khairi et al., 2015):

$$\log q_e = \log K_f + \frac{1}{n} \log C_e \tag{3}$$

In this equation, K_f represents the intercept that demonstrates the sorption capacity of the sorbents, while $1/n$ is the slope that demonstrates the sorption variation with concentration.

Langergen's first order rate model was used to describe the sorption kinetic data of β-carotene, and the equation involved is shown below (Zhang et al., 2017; Rahman et al., 2017):

$$\ln (q_e - q_t) = \ln (q_e) - K_1 t \tag{4}$$

where K_1 (min^{-1}) represents the rate constant for the pseudo-first order sorption, q_t stands for the quantity of β-carotene sorption (mg g^{-1}) during times t (min), and q_e stands for the quantity of β-carotene sorption (mg g^{-1}) during equilibrium. Furthermore, analysis of the sorption kinetic data for β-carotene was performed using the pseudo-second order equation. The basis is the adsorption equilibrium capacity, and the equation is shown below (Song et al., 2015):

$$\frac{t}{q_t} = \frac{1}{K_2 q_e^2} + \frac{t}{q_e} \tag{5}$$

The t/q_t versus t plot must generate a straight line if it can apply the second order kinetics. Furthermore, the computation of the q_e and K_2 values can be done using the slope and the intercept of the plot, respectively. It is more likely for the model to predict the kinetic behaviour of sorption, with the rate-controlling step being the chemical sorption.

Table 1 Langmuir and Freundlich constants for adsorption of β-carotene on MIP-β-CD-9VC.

q_e(exp)	Langmuir constants			Freundlich constants		
	Q_m	b	R^2	K_F	b_F	R^2
0.0268	0.04	1.838	0.987	0.027	0.704	0.969

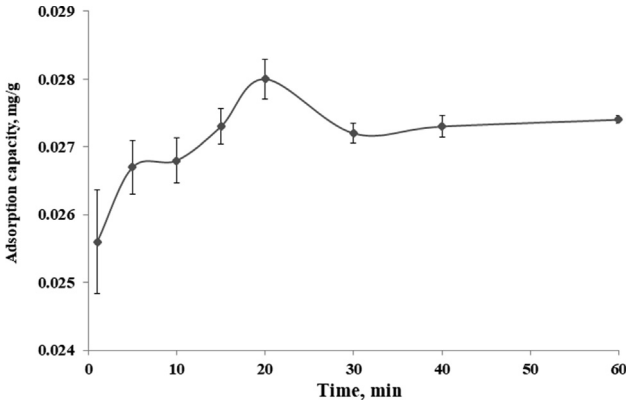

Fig. 8 Time-dependent adsorption of β-carotene on the MIP-β-CD-9VC (Experimental conditions: pH 2; POME concentration solution, 2.5 mg L^{-1}; polymer dosage, 500 mg).

3. Results and discussion

3.1. Physical characterizations of MIP-β-CD-9VC and NIP-β-CD-9VC

3.1.1. FTIR spectra of MIP-β-CD-9VC and NIP-β-CD-9VC

The FTIR spectra for β-carotene, monomer β-CD, monomer 9VC, MIP-β-CD-9VC, and NIP-β-CD-9VC were given in Fig. 1. The spectra shows a weak band of C–H stretching at 2916 cm^{-1} for β-carotene, 2924 cm^{-1} for monomer β-CD, 3043 cm^{-1} for monomer 9VC and 2927 cm^{-1} for NIP-β-CD-9VC. No peak was observed for C–H stretching in MIP-β-CD-9VC. The O–H stretching for the β-CD molecule was attributed to the peak at 3302 cm^{-1}, while MIP-β-CD-9VC and NIP-β-CD-9VC showed a low intensity of O–H group at 3379 cm^{-1} and 3356 cm^{-1}, respectively. The low intensity of O–H group might be associated to the complete polymerization of MIP-β-CD-9VC and NIP-β-CD-9VC. Two significant peaks at around 1695 cm^{-1} and 1211 cm^{-1} ascribed to the C = O and C–O stretching in MIP-β-CD-9VC and NIP-β-CD-9VC which support the existence of TDI as cross-linker. A strong band at 1637 cm^{-1} could be assigned to C = C stretch vibrations in pure monomer-9VC. However, the intensity of this vibration band in MIP-β-CD-9VC and NIP-β-CD-9VC were weak and almost disappeared which might be related to complete polymerization. The C–N stretching absorption was observed at 1159 cm^{-1}, 1058 cm^{-1} and 1095 cm^{-1} in monomer-9VC, MIP-β-CD-9VC and NIP-9VC, respectively. This peak almost overlapped with C–O absorption.

3.1.2. Field emission scanning electron microscopy (FESEM)

Fig. 2 shows a FESEM image under magnification of 25,000 for NIP-β-CD-9VC and MIP-β-CD-9VC. The morphology of MIP (Fig. 2a) shows rough surface indicated the MIP-β-CD-9VC has certain binding sites produced in the polymer network during the polymerization process. A smooth and irregular surface in NIP-β-CD-9VC (Fig. 2b) was due to the fact that there is no specific binding sites had been created for the polymer.

3.1.3. Thermal stability

TGA analysis was performed to determine the decomposition and thermal stability of the MIP and NIP under certain conditions. Fig. 3 shows the thermogram data of MIP-β-CD-9VC and NIP-β-CD-9VC particles, respectively. The similar kind of degradation pattern were observed for thermograms of MIP-β-CD-9VC and NIP-β-CD9VC. The MIP-β-CD-9VC started to decompose, T_i at 80 °C with 6% weight loss and shows final decomposition, T_f at 320 °C with 66.7% weight loss. Meanwhile, NIP-β-CD-9VC started to decompose T_i at 111 °C with 23.5% weight loss and displays final decomposition T_f at 314 °C with 54.5%. This indicates, MIP-β-CD-9VC has higher thermal stability compared to NIP-β-CD-9VC due to the monomer template complex which formed in MIP network during polymerization process.

3.2. Adsorption studies

3.2.1. Effect of pH

The optimum pH was done by determining the effect of different pH towards adsorption capacity of β-carotene. The contact time (20 min), concentration of POME solution (2.5 mg L^{-1}) and polymer dosage (500 mg) were kept constant while pH of POME solution was changed. Fig. 4 shows the effect of different pH for adsorption of β-carotene by MIP-β-CD-9VC and NIP-β-CD-9VC. It can be observed that, the adsorption

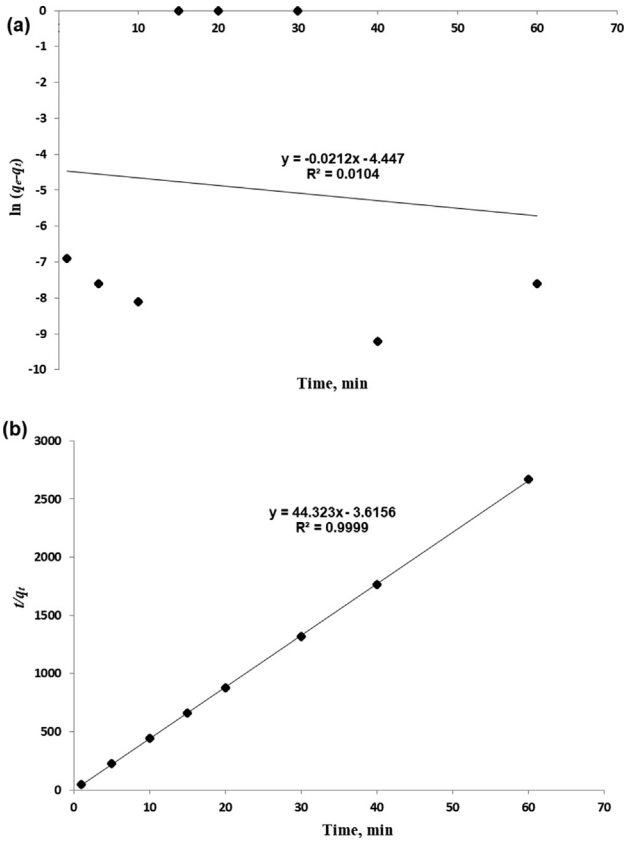

Fig. 9 (a) Pseudo-first order and (b) Pseudo-second order kinetic models for adsorption of β-carotene on MIP-β-CD-9VC. (Experimental conditions: pH 2; POME concentration solution, 2.5 mg L^{-1}; polymer dosage, 500 mg; contact time, 20 min).

Table 2 The first order and second order kinetic constants for the MIP-β-CD-9VC.

q_e(exp) mg g^{-1}	First-order			Second-order		
	K_1 (min^{-1})	q_e(calc) (mg g^{-1})	R^2	K_2 (g $mg^{-1}min^{-1}$)	q_e(calc) (mg g^{-1})	R^2
0.028	0.0256	0.004	0.0414	0.0714	0.0274	0.9999

capacity of β-carotene decreased slightly in pH range of 2 to 9 for both MIP-β-CD-9VC and NIP-β-CD-9VC. The adsorption capacity of β-carotene by NIP-β-CD-9VC was lower than MIP-β-CD-9VC which is due to non-specific interaction with the polymer matrix (Yang et al, 2009). Hence, pH 2 has been selected as optimum pH for optimizing further analysis.

3.2.2. Effect of dosage

The study was performed using various amounts of MIP-β-CD-9VC, ranging from 50 to 500 mg, while keeping other parameters constant (pH 2, contact time = 20 min, concentration of POME solution = 2.5 mg L^{-1}). As shown in Fig. 5, the percentage removal of β-carotene increased by increasing the MIP dosage due to the more surface available for adsorption to occur, as number of available active adsorption sites in the MIP-β-CD-9VC (Oguntimein, 2015; Yusof et al., 2013). The maximum removal efficiency (91.1%) was achieved at a polymer dosage of 500 mg. Dosage of 500 mg was considered as optimum dosage for optimizing further analysis.

3.2.3. Isotherm study

Measurement of the sorption isotherm for β-carotene was done using MIP-β-CD-9VC. POME was diluted into varying concentrations from 0.1 to 2.5 mg L^{-1}. Other parameter were kept constant (pH 2, contact time = 20 min, polymer dosage = 500 mg) while concentration of POME solution was changed. As shown in Fig. 6, the adsorption capacity increased with increasing of the β-carotene concentration in POME. The maximum of adsorption capacity was observed at concentration of 2.5 mg L^{-1}. Therefore, 2.5 mg L^{-1} has been selected as the optimum concentration of POME solution for further analysis.

Fig. 7 shows the (a) Langmuir and (b) Freundlich models for the adsorption of β-carotene by MIP-β-CD-9VC. The Langmuir model has higher correlation coefficient R^2. The correlation coefficient R^2 for the Langmuir model is 0.987 and Freundlich model is 0.9688. However, the value of calculated Q_m for Langmuir model is not comparable to the q_e experimental value. The Q_m for Langmuir model is 0.04 and q_e experimental value is 0.0268, while the value of calculated K_f for Freundlich model is quite close to the q_e experimental value which indicates that the adsorption of β-carotene by MIP-β-CD-9VC follows the Freundlich isotherm. The values of Langmuir and Freundlich constants for the MIP-β-CD-9VC were summarized in Table 1.

3.2.4. Kinetic study

Fig. 8 shows β-carotene adsorption by MIP-β-CD-9VC under varying adsorption times, from 1 to 60 min while keeping other parameters constant (pH 2, polymer dosage = 500 mg, concentration of POME solution = 2.5 mg L^{-1}). Referring to the Fig. 8, the maximum β-carotene adsorption by MIP-β-CD-9VC is 0.028 mg g^{-1}. The adsorption capacity of β-carotene increased by increasing the adsorption time up to 20 min. Then the adsorption capacity of β-carotene decreased and eventually reached a plateau after 30 min. Adsorption time at 20 min has been considered as optimum contact time on the removal process.

Fig. 9 shows that the pseudo second order model has higher correlation coefficient R^2 = 0.9999 compared to the lower correlation coefficient R^2 = 0.0104 of the Pseudo first order model. Moreover, the rate constant values that are summarized in Table 2 offer information about the theoretical value of q_e (cal) and how it is closer in value to the experimental q_e (exp) for the pseudo-second order. Nevertheless, pseudo first order has exhibited differences between calculated and experimental sorption capacities. Thus, it is apparent that the pseudo-second order kinetic model offered good correlation for β-carotene sorption onto MIP-β-CD-9VC.

3.2.5. Reusability study

Reusability studies were investigated in order to determine the stability and regeneration of the MIP-β-CD-9VC. The MIP-β-CD-9VC was repeatedly used to remove β-carotene from POME at optimal conditions (pH 2, contact time = 20 min, polymer dosage = 500 mg, concentration of POME solution = 2.5 mg L^{-1}). The performance of adsorption capacities for MIP-β-CD-9VC is shown in Fig. 10. The adsorption capacity of MIP decreased from 0.0278 mg g^{-1} to 0.0257 mg g^{-1}. The decrease of adsorption capacity might be related to *n*-hexane solvent used to extract the β-carotene from the cavities. The washing conditions might result in destruction or collapse of some binding sites in the MIPs.

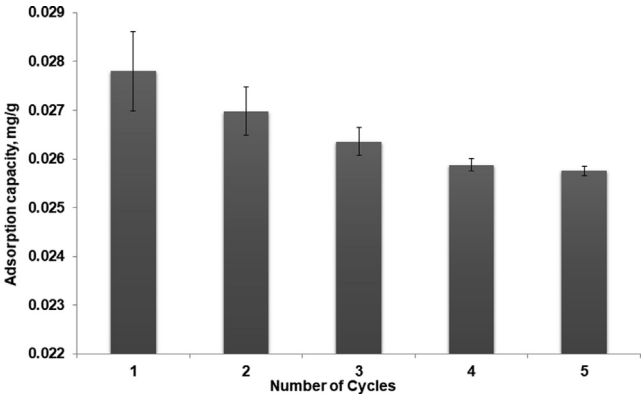

Fig. 10 Reusability of MIP-β-CD-9VC (Experimental conditions: pH 2; POME concentration solution, 2.5 mg L^{-1}; polymer dosage, 500 mg; contact time, 20 min).

4. Conclusion

MIP-β-CD-9VC has been synthesized by bulk polymerization method and evaluated using kinetic model which follows a pseudo–second–order kinetic. Equilibrium data fitted well with the Freundlich model. It was observed that, the binding capacity for β-carotene by MIP-β-CD-9VC was higher than NIP-β-CD-9VC. Optimal conditions of pH 2, POME concentration of 2.5 mg L^{-1}, polymer dosage of 500 mg and contact time of 20 min were obtained in this study. The prepared MIP-β-CD-9VC have been applied successfully for the adsorptive removal of β-carotene from POME solution and optimized.

Declaration of Competing Interest

The authors declare that they have no known competing financial interests or personal relationships that could have appeared to influence the work reported in this paper.

Acknowledgements

The authors would like to thank Universiti Putra Malaysia for financial support throughout this project. W.M.A. acknowledges the Embassy of the State of Libya for financial support. This work was supported by the Ministry of Higher Education (MOHE), Malaysia [grant numbers 9590600] in the form of Prototype Research Grant Scheme (PRGS).

References

Abdulsalam, M., Man, H.C., Yunos, K.F., Abidin, Z.Z., Idris, A.I., Hamzah, M.H., 2020. Augmented yeast-extract and diary-waste for enhancing bio-decolourization of palm oil mill effluent using activated sludge. J. Water Process. Eng. 36,. https://doi.org/10.1016/j.jwpe.2020.101263 101263.

Ahmed, Y., Yaakob, Z., Akhtar, P., Sopian, K., 2015. Production of biogas and performance evaluation of existing treatment processes in palm oil mill effluent (POME). Renew. Sustain. Energ. Rev. 42, 1260–1278. https://doi.org/10.1016/j.rser.2014.10.073.

Azizi, A., Christina, S., Bottaro, 2020. A critical review of molecularly imprinted polymers for the analysis of organic pollutants in environmental water samples. J. Chromatogr. A 1614,. https://doi.org/10.1016/j.chroma.2019.460603 460603.

Aziz, M.M.A., Kassim, K.A., El Sergany, M., Anuar, S., Jorat, M.E., Yaacob, H., Ahsan, A., Imteaz, M.A., Arifuzzaman, 2020. Recent advances on palm oil mill effluent (POME) pretreatment and anaerobic reactor for sustainable biogas production. Renew. Sustain. Energ. Rev. 119, 109603. https://doi.org/10.1016/j.rser.2019.109603

Bello, M.M., Nourouzi, M.M., Abdullah, L.C., Choong, T.S.Y., Koay, Y.S., Keshani, S., 2013. POME is treated for removal of color from biologically treated POME in fixed bed column: Applying wavelet neural network (WNN). J. Hazard. Mater. 262, 106–113. https://doi.org/10.1016/j.jhazmat.2013.06.053.

Choong, T.S.Y., Chuah, T.G., Yunus, R., Yap, Y.H.T., 2010. Adsorption of β-carotene onto mesoporous carbon coated monolith in isopropyl alcohol and n-hexane solution : equilibrium and thermodynamic study. Chem. Eng. J. 164, 178–182. https://doi.org/10.1016/j.cej.2010.08.052.

Hassan, S., Sayour, H., Azab, W.E., Mansour, M., 2016. Synthesis and characterization of molecularly imprinted nanoparticle polymers for selective separation of Anthracene. J. Disper. Sci. Technol. 37, 1241–1251. https://doi.org/10.1080/01932691.2015.1089514.

Hegazy, E.A., Sabry, G.M., Ezz, M.K., Kamal, H., Lotfy, S., Mansour, S.Z., Eissa, D.H., 2016. Radiation synthesis and characterization of cholesterol molecularly imprinted polymer of crosslinked hydroxyethyl methacrylate. Int. J. Sci. Res. 5, 297–302.

Jasni, J., Arisht, S.N., M-Yasin, N.H., Abdul, P.M., Linc, S.K., Liuc, C.M., Wuc, S.Y., M-Jahim, J., Takriff, M.S., 2020. Comparative toxicity effect of organic and inorganic substances in palm oil mill effluent (POME) using native microalgae species. J. Water Process Eng. 34,. https://doi.org/10.1016/j.jwpe.2020.101165 101165.

Khairi, N.A.S., Yusof, N.A., Abdullah, A.H., 2015. Removal of toxic mercury from petroleum oil by newly synthesized molecularly-imprinted polymer. Int. J. Mol. Sci. 16, 10562–10577. https://doi.org/10.3390/ijms160510562.

Lafarge, C., Bitar, M., Hosry, L.E., Cayot, P., B-Maroun, E., 2020. Comparison of molecularly imprinted polymers (MIP) and sol–gel molecularly imprinted silica (MIS) for fungicide in a hydro alcoholic solution. Mater. Today Commun. 24,. https://doi.org/10.1016/j.mtcomm.2020.101157 101157.

Mosbach, K., Ramstrom, O., 1996. The emerging technique of molecular imprinting and its future impact on biotechnology. Bio-Technol. 14, 163–170.

Ncube, S., Kunene, P., Tavengwa, N.T., Tutu, H., Richards, H., Cukrowska, E., Chimuka, L., 2017. Synthesis and characterization of a molecularly imprinted polymer for the isolation of the 16 US-EPA priority polycyclic aromatic hydrocarbons (PAHs) in solution. J. Environ. Manage. 199, 192–200. https://doi.org/10.1016/j.jenvman.2017.05.041.

Neoh, C.H., Lam, C.Y., Lim, C.K., Yahya, A., Ibrahim, Z., 2014. Decolourization of palm oil mill effluent using growing cultures of *Curvularia clavata*. Environ. Sci. Pollut. Res. 21, 4397–4408. https://doi.org/10.1007/s11356-013-2350-1.

Oguntimein, G.B., 2015. Biosorption of dye from textile wastewater effluent onto alkali treated dried sunflower seed hull and design of a batch adsorber. J. Environ. Chem. Eng. 3, 2647–2661. https://doi.org/10.1016/j.jece.2015.09.028.

Rahman, S.K.A., Yusof, N.A., Abdullah, A.H., Mohammad, F., Idris, A., Al-lohedan, H.A., 2018. Evaluation of porogen factors for the preparation of ion imprinted polymer monoliths used in mercury removal. PLoS ONE 13, 1–14. https://doi.org/10.1371/journal.pone.0195546.

Rahman, S.K.A., Yusof, N.A., Mohammad, F., Abdullah, A.H., Idris, A., 2017. Ion imprinted polymer monoliths as adsorbent materials for the removal of Hg (II) from real-time aqueous samples. Curr. Sci. 113, 2282–2291.

Ratpukdi, T., 2012. Decolorization of anaerobically treated palm oil mill wastewater using combined coagulation and vacuum ultraviolet-hydrogen peroxide. Int. J. Chem. Eng. Appl. 3 (2012), 333–336. https://doi.org/10.7763/IJCEA.2012.V3.212.

Song, R., Hu, X., Guan, P., Li, J., Qian, L., Wang, C., Wang, Q., 2015. Synthesis of porous molecularly imprinted polymers for selective adsorption of glutathione. Appl. Surf. Sci. 332, 159–166. https://doi.org/10.1016/j.apsusc.2015.01.165.

Speltini, A., Scalabrini, A., Maraschi, F., Sturini, M., Profumo, A., 2017. Newest applications of molecularly imprinted polymers for extraction of contaminants from environmental and food matrices : A review. Anal. Chim. Acta 974, 1–26. https://doi.org/10.1016/j.aca.2017.04.042.

Tabassum, S., Zhang, Y., Zhang, Z., 2015. An integrated method for palm oil mill effluent (POME) treatment for achieving zero liquid discharge - A pilot study. J. Clean. Prod. 95, 148–155. https://doi.org/10.1016/j.jclepro.2015.02.056.

Wang, X., Pei, Y., Hou, Y., Pei, Z., 2019. Fabrication of core-shell magnetic molecularly imprinted nanospheres towards hypericin via click polymerization. Polymers 11, 313. https://doi.org/10.3390/polym11020313.

Wu, T.Y., Mohammad, A.W., Jahim, J., Anuar, N., 2007. Palm oil mill effluent (POME) treatment and bioresources recovery using ultrafiltration membrane: Effect of pressure on membrane fouling.

Biochem. Eng. J. 35, 309–317. https://doi.org/10.1016/j.bej.2007.01.029.

Yan, H., Row, K.H., 2006. Characteristic and synthetic approach of molecularly imprinted polymer. Int. J. Mol. Sci. 7, 155–178. https://doi.org/10.3390/i7050155.

Yang, H.H., Zhou, W.H., Guo, X.C., Chen, H.Q., Zhao, H.Q., 2009. Molecularly imprinted polymer as SPE sorbent for selective extraction of melamine in dairy products. Talanta 80, 821–825.

Yusof, N.A., Rahman, S.K.A., Hussein, M.Z., Ibrahim, N.A., 2013. Preparation and characterization of molecularly imprinted polymer as SPE sorbent for melamine isolation. Polymers 5, 1215–1228. https://doi.org/10.3390/polym5041215.

Zahrim, A., 2014. Palm oil mill biogas producing process effluent treatment: A short review. J. Appl. Sci. 14, 3149–3155. https://doi.org/10.3923/jas.2014.3149.3155.

Zhang, J., Liu, D., Shi, Y., Sun, C., Niu, M., Wang, R., Hu, F., Xiao, D., He, H., 2017. Determination of quinolones in wastewater by porous β-cyclodextrin polymer based solid-phase extraction coupled with HPLC. J. Chromatogr. B 1068–1069, 24–32. https://doi.org/10.1016/j.jchromb.2017.09.046.